

BIBECHANA

A Multidisciplinary Journal of Science, Technology and Mathematics

ISSN 2091-0762 (Print), 2382-5340 (Online)

Journal homepage: <http://nepjol.info/index.php/BIBECHANA>

Publisher: Research Council of Science and Technology, Biratnagar, Nepal

Modeling equations to predict the mixing behaviour of Al–Fe liquid alloy at different temperatures

S. K. Yadav^{1,2*}, L. N. Jha², D. Adhikari^{3*}

¹Department of Physics, Suryanarayan Satyanarayan Morbaita Yadav Multiple Campus, Tribhuvan University, Siraha, Nepal.

²Central Department of Physics, Tribhuvan University, Kirtipur, Nepal.

³Department of Physics, Mahendra Morang Adarsh Multiple Campus, Tribhuvan University, Biratnagar, Nepal.

*E-mail: yadavshashit@yahoo.com

Article history: Received 05 October, 2017; Accepted 20 November, 2017

DOI: <http://dx.doi.org/10.3126/bibechana.v15i0.18624>

This work is licensed under the Creative Commons CC BY-NC License. <https://creativecommons.org/licenses/by-nc/4.0/>



Abstract

Redlich–Kister (R–K) polynomials have been associated with the extended regular associated solution model to predict and explain the thermodynamic properties and structural properties of Al–Fe liquid alloy at 1873 K, 1973 K, 2073 K and 2173 K; 1873 K being its melting temperature. The thermodynamic properties, such as free energy of mixing (G_M) and activities of free monomers (a_{Al} and a_{Fe}) and structural properties, such as concentration fluctuation in long wave length limit ($S_{CC}(0)$), chemical short range order parameter (α_1) and ratio of diffusion coefficients (D_M/D_{id}) have been predicted at above stated temperatures. Renovated Butler model has been employed to predict the surface tension (σ) and surface segregation (x^S) of the alloy at stated temperatures with the help of thermodynamic properties. Theoretical findings prevail that the tendency towards compound formation of the liquid alloy decreases with increase in its temperature beyond melting temperature. Eventually, its surface tension decreases and there is gradual exchange of atoms between the surface and bulk regions to maintain equilibrium at elevated temperatures. The liquid alloy under investigation thus shows ideal behaviours at higher temperatures.

Keywords: R–K polynomials; Thermodynamic properties; Surface segregation; ideal behaviour.

1. Introduction

Alloying phenomena have been developed as one of the robust tool to achieve desired materials with required characteristics. Though alloys have profound utilizations in the solid state, they are fabricated near to the melting temperatures of the constituent atoms. The comprehensive knowledge of the thermodynamics of the initial melt is thus imperative to explain the mixing behaviours of the subsystems. This information cannot be solely achieved from experiments as being cumbersome facing adversities associated with the high reactivity of metals at elevated temperatures. In this limelight, the devising of theoretical models to explain the mixing behaviours of the alloy melts at a

temperature and extrapolating at different temperatures are mandatory. Several theoretical models [1–9] so far have been tooled to understand and explain the energetic of the liquid alloys. In this work, we intend to predict the thermodynamic and structural properties of Al–Fe liquid alloy at different temperatures by extending regular associated solution model [5, 7, 9–12]. Moreover, the thermodynamic properties at different temperatures have been correlated with Renovated Butler model [13–15] to predict the surface properties of the liquid alloy at different temperatures.

When the atoms of type A (=Al) and B (=Fe) are mixed near to their melting temperature, there are preferable associations of the types AA, BB and AB in the framework of regular associated solution model. It is assumed that there exist unequal interactions among the associated and unassociated atoms. The expressions for the thermodynamic and structural properties of the liquid melt are derived on this fundamental. The details about the model can be found from references 5, 7 and 9 (also see ref. 15). The model parameters of most of the theoretical models are just fitting parameters to establish the equivalence between the computed and observed thermodynamic properties. But the model fit parameters of the preferred model (regular associated solution model) are determined from the experimental values of the activity coefficients of the monomers of the liquid alloys at infinite dilutions. Also the mole fractions of the associated complex and unassociated atoms can be computed in the preferred model regardless of other models. With this regard, the regular associated model has been extended to predict the thermodynamic and structural properties of the considered system at different temperatures. Accordingly, R–K polynomials [16, 17] have been associated with these procedures to determine the fitting coefficients. Moreover, the importance of the Al–Fe liquid alloys is mentioned in ref. 16. Among the different stable chemical complexes, we have assumed Al₃Fe as one of the most energetically favoured complex at 1873 K and have considered for further study [18, 19].

The details of the methodology containing basic formulations are mentioned in the Section 2, results and discussion are amended in the Section 3 and the Section 4 contains the conclusions of the present work.

2. Methodology

2.1 Thermodynamic Properties

Assume the chemical complex of type A_μB_ν (A_μB_ν ⇌ μA + νB) exists in a mole of binary solution, where A (=Al), B (=Fe) and μ (=3) and ν (=1) are small integers whose values are determined from the compound forming concentration in the solid state. The true mole fractions of free monomers A (x_A) and B (x_B) are then given as [5, 11, 18]

$$x_A = x_1 - \mu x_2 x_{A_\mu B} \quad \text{and} \quad x_B = x_2 - (1 - \mu x_2) x_{A_\mu B} \quad (1)$$

where x₁ and x₂ are the gross mole fractions of atoms A and B respectively and x_{A_μB_ν} is the true mole fraction of the complex.

The activity coefficients of monomers (γ_A and γ_B) and complex (γ_{A_μB_ν}) can be expressed in terms of pairwise interaction energies as

$$RT \ln \gamma_A = x_B^2 \omega_{12} + x_{A_\mu B}^2 \omega_{13} + x_B x_{A_\mu B} (\omega_{12} - \omega_{23} + \omega_{13}) \quad (2a)$$

$$RT \ln \gamma_B = x_{A_\mu B}^2 \omega_{23} + x_A^2 \omega_{12} + x_A x_{A_\mu B} (\omega_{23} - \omega_{13} + \omega_{12}) \quad (2b)$$

$$RT \ln \gamma_{A_\mu B} = x_A^2 \omega_{13} + x_B^2 \omega_{23} + x_A x_B (\omega_{13} - \omega_{12} + \omega_{23}) \quad (2c)$$

where T is temperature in absolute scale and R is the universal gas constant. The terms ω₁₂, ω₁₃ and ω₂₃ represent the pairwise interaction energies for the species A, B; A, A_μB and B, A_μB respectively. ω₁₂ and ω₁₃ in terms with activity coefficients at infinite dilution (γ₁⁰, 1=A and γ₂⁰, 2=B) can be correlated as follows [11, 15]

$$\ln \gamma_1^0 = \frac{\omega_{12}}{RT} \quad (3a)$$

$$k \exp\left(\frac{\omega_{13}}{RT}\right) = \frac{\gamma_1^0 \gamma_2^0}{\gamma_1^0 - \gamma_2^0} \quad (3b)$$

where k is the equilibrium constant for the above mentioned chemical reaction and is given as

$$\begin{aligned} \ln k = & \ln\left(\frac{x_A^\mu x_B}{x_{A\mu B}^\mu}\right) + \frac{\omega_{12}}{RT} [\mu x_B(1 - x_A) + x_A] + \frac{\omega_{13}}{RT} [\mu x_{A\mu B}(1 - x_A) - x_A] \\ & + \frac{\omega_{23}}{RT} [x_{A\mu B}(1 - \mu x_B) - x_B] \end{aligned} \quad (4)$$

In regular associated solution model, it is assumed that $x_1 \gamma_1 = x_A \gamma_A$ and $x_2 \gamma_2 = x_B \gamma_B$ where γ_1 and γ_2 are the respective gross activity coefficients of monomers 1 and 2 respectively. One can, therefore, obtain the following relations [11, 20]

$$\ln \gamma_1 = \ln \gamma_A + \ln\left(\frac{x_A}{x_1}\right) \quad \text{and} \quad \ln \gamma_2 = \ln \gamma_B + \ln\left(\frac{x_B}{x_2}\right) \quad (5)$$

On solving Equations (2a) and (2b), yields

$$\frac{\omega_{13}}{RT} = \frac{x_B \ln\left(\frac{\alpha_2}{x_B}\right) + (1 - x_B) \ln\left(\frac{\alpha_1}{x_A}\right) - x_B(1 - x_B) \frac{\omega_{12}}{RT}}{x_{A\mu B}^2} \quad (6a)$$

$$\frac{\omega_{23}}{RT} = \frac{x_A \ln\left(\frac{\alpha_1}{x_A}\right) + (1 - x_A) \ln\left(\frac{\alpha_2}{x_B}\right) - x_A(1 - x_A) \frac{\omega_{12}}{RT}}{x_{A\mu B}^2} \quad (6b)$$

where α_1 and α_2 are the activities of A and B respectively. Using Equations (4) and (6), the mole fraction of the complex and the unassociated atoms can be expressed by the relation [5, 7]

$$\ln k + \frac{\omega_{13}}{RT} = \left(\frac{1+x_A}{x_{A\mu B}}\right) \ln\left(\frac{\alpha_1}{x_A}\right) + \frac{x_B}{x_{A\mu B}} \left[\ln\left(\frac{\alpha_1}{x_A}\right) - \frac{\omega_{12}}{RT}\right] + \ln\left(\frac{a_1^\mu a_2}{x_{A\mu B}}\right) \quad (7)$$

Using above relations, the expression for the free energy of mixing ($\frac{G_M}{RT}$) can be obtained as [11]

$$\begin{aligned} \frac{G_M}{RT} = & \frac{1}{1 + \mu x_{A\mu B}} RT \left[\left(x_A x_B \frac{\omega_{12}}{RT} + x_A x_{A\mu B} \frac{\omega_{13}}{RT} + x_B x_{A\mu B} \frac{\omega_{23}}{RT} \right) \right. \\ & \left. + (x_A \ln x_A + x \ln x_B + x_{A\mu B} \ln x_{A\mu B}) + x_{A\mu B} \ln k \right] \end{aligned} \quad (8)$$

2.2 Structural Properties

Concentration fluctuation in the long wavelength limit ($S_{CC}(0)$) in terms of free energy of mixing (G_M) can be given by the standard thermodynamic relation as [5, 15]

$$S_{CC}(0) = RT \left(\frac{\partial^2 G_M}{\partial x_1^2} \right)_{T,P}^{-1} \quad (9a)$$

Using Equation (8) in Equation (9a); the expression for ($S_{CC}(0)$) can be obtained as

$$S_{CC}(0) = 1 / \left[\frac{1}{1 + \mu x_{A\mu B}} \left\{ \frac{2}{RT} \left(x'_A x'_B w_{12} + x'_A x'_{A\mu B} w_{13} + x'_B x'_{A\mu B} w_{23} \right) + \left(\frac{x_A'^2}{x_A} + \frac{x_B'^2}{x_B} + \frac{x_{A\mu B}'^2}{x_{A\mu B}} \right) \right\} \right] \quad (9b)$$

where the prime denotes the differentiations with respect to concentrations and $\frac{\partial^2 G_M}{\partial x_1^2} > 0$ for $\frac{\partial G_M}{\partial x_1} = 0$. x'_A and x'_B are obtained by using Equation (1) and $x'_{A\mu B}$ is obtained using Equation (4) by using the condition $\frac{d \ln k}{dx_1} = 0$. The factor $(1 + \mu x_{A\mu B})^{-1}$, which appears as a coefficient of all terms containing x_A , x_B and $x_{A\mu B}$ in Equations (8) and (9b) is a result of change in the basis for expressing mole fractions of species A, B and $A_\mu B$ from that used for x_1 and x_2 .

Further, the degree of local ordering in the liquid binary alloy can be understood by estimating chemical short range order parameter (α_1) and in terms of $S_{CC}(0)$ is expressed as [7, 21]

$$\alpha_1 = \frac{S-1}{S(Z-1)+1}, \text{ where } S = \frac{S_{CC}(0)}{S_{CC}^{id}(0)} \quad (10)$$

where Z is the coordination number and $Z=10$ is taken for our calculation [16]. It is seen that varying the value of Z does not have any effect in on the position of the minima of α_1 but it helps to vary the depth keeping the other features unchanged.

The microscopic structural properties of binary liquid alloy can be further understood in terms of ratio of coefficients of diffusion. The ratio of diffusion coefficients (D_M/D_{id}) can be expressed in terms of $S_{CC}(0)$ by using Darken thermodynamic equation as [22]

$$\frac{D_M}{D_{id}} = \frac{x_1 x_2}{S_{CC}(0)} \quad (11)$$

where $D_M = D_{id} \partial \ln a_A / \partial x_1$ represents the chemical or mutual diffusion coefficient and D_{id} represents the intrinsic diffusion coefficient for an ideal mixture.

2.3 Surface Properties

According to Renovated Butler model, the surface tension (σ) for the A-B type liquid alloys can be given as [13-15]

$$\sigma = \sigma_i^0 + \frac{RT}{\lambda_i} \ln \left(\frac{x_{s,i}}{x_i} \right) + \frac{\Delta G_{s,i}^E - \Delta G_i^E}{\lambda_i} = \sigma_j^0 + \frac{RT}{\lambda_j} \ln \left(\frac{x_{s,j}}{x_j} \right) + \frac{\Delta G_{s,j}^E - \Delta G_j^E}{\lambda_j} \quad (12a)$$

where σ_i^0 represents the surface tension of the pure components, λ_i represents the molar surface area of component i in the liquid solution and $i=A, B$. $\Delta G_{s,i}^E$ stands for the surface partial excess free energy of the components, ΔG_i^E stands for the bulk partial free energy of the components, x_i represents the bulk mole fraction of the components and $x_{s,i}$ represents the surface mole fraction of the components and $x_{s,i} + x_{s,j} = 1$.

The molar surface area of a pure liquid metal i is computed by the relation

$$\lambda_i = f(V_i^0)^{2/3} (N_{AV})^{1/3} \quad (12b)$$

where $N_{AV} (=6.022 \times 10^{23} \text{ mol}^{-1})$ is the Avogadro's number, V_i^0 is the molar volume of pure metal i at the melting temperature and f is the geometrical constant which is given as

$$f = \left(\frac{3f_b}{4} \right)^{2/3} \frac{\pi^{1/3}}{f_s} \quad (12c)$$

where f_b and f_s are the volume and surface packing fractions. The values of f_b and f_s depends upon the type of crystal structure of the pure components of the liquid alloys.

3. Results and Discussion

3.1 Thermodynamic Properties

The model fit parameters (ω_{12} , ω_{13} , ω_{23} , $x_{A=Al}$, $x_{B=Fe}$, $x_{A\mu B=Al_3Fe}$ and k) for Al-Fe melt at 1873 K are evaluated using Equations (1), (3), (4), (6) and (7) with the aid of observed essential ingredients [19]. The initial values of these input parameters as well as the temperature derivative terms of pairwise interaction energies ($\partial \omega_{12} / \partial T$, $\partial \omega_{13} / \partial T$ and $\partial \omega_{23} / \partial T$) are taken from ref. 18. The extension of the regular associated solution model has been made by considering that the parameters, such as x_A , x_B , $x_{A\mu B}$, k , $\partial \omega_{12} / \partial T$, $\partial \omega_{13} / \partial T$ and $\partial \omega_{23} / \partial T$ remain constant with increase in the temperature of the system above its melting temperature. We have computed the mixing behaviors of the alloy at 1873 K, 1973 K, 2073 K and 2173 K, 1873 K being its melting temperature. The parameters ω_{12} , ω_{13} and ω_{23} in the preferred model are assumed to be temperature dependent only and they are computed using the following relations [15, 23]

$$d[\omega_{i,j}(T)]_{x_p} = (\partial\omega_{i,j}/\partial T)dT \text{ and } \omega_{i,j}(T_k) = \omega_{i,j}(T) + (\partial\omega_{i,j}/\partial T)dT \quad (13)$$

where $i, j = 1, 2$ and 3 for $i \neq j$, x_p is the bulk mole fraction of A or B such that $p = 1$ or 2 and $dT = T_k - T$; T ($=1873$ K) is the melting temperature and T_k ($=1973$ K, 2073 K and 2173 K) are the temperature of interests for the alloy.

The activity coefficients as a function of concentration for the unassociated atoms of Al and Fe of the liquid alloy are then computed at different temperatures using Equations (2a) and (2b). Eventually, the compositional dependence of excess free energy of mixing (G_M^{XS}) of the liquid alloy are predicted at such temperatures on the floor of which R–K polynomials are fitted.

The excess free energy of mixing as a function of concentration is given by a polynomial, such as R–K polynomial [16, 17] as

$$G_M^{XS}(x, T) = x_1 x_2 \sum_{l=0}^m K_l(T)(x_1 - x_2)^l \quad (14a)$$

with $K_l(T) = A_l + B_l T + C_l T \ln T + D_l T^2 + \dots$; where K_l has the same temperature dependence as G_M^{XS} and A, B, C and D are the coefficients to be determined. The partial excess free energies of components of the alloy are given as

$$G_A^{XS}(x, T) = x_2^2 \sum_{l=0}^m K_l(T)[(1 + 2l)x_1 - x_2](x_1 - x_2)^{l-1} \quad (14b)$$

$$G_B^{XS}(x, T) = x_1^2 \sum_{l=0}^m K_l(T)[x_1 - x_2(1 + 2l)](x_1 - x_2)^{l-1} \quad (14c)$$

The optimized coefficients are obtained by the method of least square fitting using programming in computer software Microsoft Excel 2007 and are tabulated in the Table 1.

Table 1: Optimized coefficient set of G_M^{XS} for Al–Fe liquid alloy

l	$A_l(\text{J mol}^{-1})$	$B_l(\text{J mol}^{-1}\text{K}^{-1})$	$C_l(\text{J mol}^{-1}\text{K}^{-1})$	$D_l(\text{J mol}^{-1}\text{K}^{-2})$
0	-65932.40	0.7591290	1.225507	-0.0003400
1	-140.5359	-6.861770	7.28×10^{-12}	-5.00×10^{-6}
2	-342.6730	-9.319690	-0.4085	9.86×10^{-5}
3	-486.8970	-4.731690	-0.4085	9.86×10^{-5}

The compositional dependence of excess free energy of mixing at different temperatures computed from Equation (14a) using the values in table 1 are plotted in Figure 1. It can be observed that G_M^{XS} gradually decreases at elevated temperatures. It can, therefore, be forecasted that the complex formation tendency of the liquid alloy is the maximum at its melting temperature and gradually decreases at elevated temperatures.

Once the partial excess free energies of A and B are obtained, the activity coefficients at different temperatures are computed using the relation $G_p^{XS} = RT \sum \ln \gamma_p$, where the terms carry their usual meanings. The compositional dependence of the activities of A (a_{Al}) and B (a_{Fe}) are then computed from Equation (5) and are plotted in Figure 2. It can be observed that the activities of the free monomers gradually increase with increase in the temperature of the alloy predicting the similar tendency as by G_M above. Similar results are predicted and explained by other researches [17, 23–25] for different alloy systems employing different techniques.

3.2 Structural Properties

The tendency towards complex formation and the local arrangements of atoms in the initial melt of the liquid systems can be further analyzed in terms of $S_{CC}(0)$, α_1 and D_M/D_{id} . At a temperature and a concentration if $S_{CC}(0) < S_{CC}^{id}(0)$ for which $\alpha_1 < 0$ and $D_M/D_{id} > 1$, then there is favourable association

between the unlike atoms of the form A–B called ordering. Additionally, at such conditions if $S_{CC}(0) > S_{CC}^{id}(0)$ for which $\alpha_1 > 0$ and $D_M/D_{id} < 1$, then the association between the like atoms of form A–A or B–B is favoured in the melt called segregating.

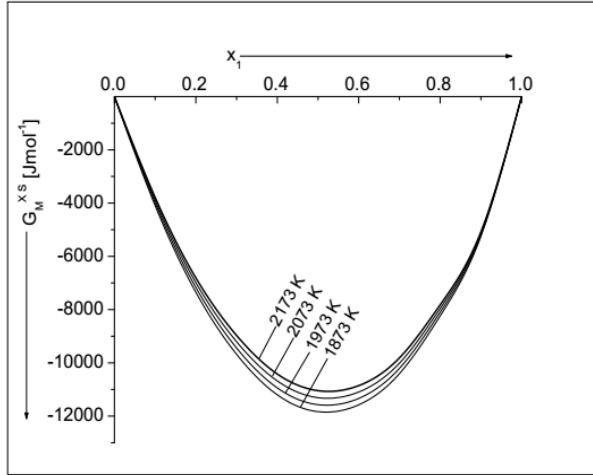


Fig. 1: Excess free energy of mixing (G_M^{XS}) as a function of concentration of Al (x_1) for Al–Fe liquid alloy at different temperatures.

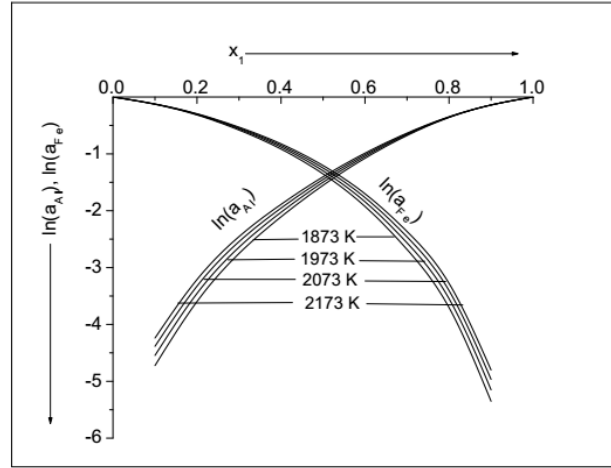


Fig. 2: Activities of Al ($\ln(a_{Al})$) and Fe ($\ln(a_{Fe})$) as a function of concentration of Al (x_1) for Al–Fe liquid alloy at different temperatures.

Figure 3 shows the compositional dependence of $S_{CC}(0)$ for the alloy at different temperatures computed from Equation (9) with the aid of above determined model parameters. The predicted theoretical values of $S_{CC}(0)$ gradually increases and get closure to their corresponding ideal values at elevated temperatures. The deviation between the ideal and theoretical values of $S_{CC}(0)$ at complex formation concentration ($x_{CC} = x_1 = 0.75$) are 0.1121, 0.1093, 0.1065 and 0.1038 at temperatures 1873 K, 1973 K, 2073 K and 2173 K respectively forecasting that the tendency towards the complex formation is the most at 1873 K which is its melting temperature and the least at 2173 K. Theoretical investigations thus predict that the preferred system is the most interacting at 1873 K and the least at 2173 K.

The compositional dependence of α_1 and D_M/D_{id} at different temperatures are computed from Equations (10) and (11) and are portrayed in Figure 4. It can be observed that the plots of α_1 gradually shallows with increase in the temperature of the alloy predicting the decrease in the compound forming tendency at elevated temperatures. The computed values of α_1 at compound forming concentration are -0.1298, -0.1228, -0.1164 and -0.1103 at 1873 K, 1973 K, 2073 K and 2173 K respectively. The perusal of Figure 5 indicates that computed values of D_M/D_{id} gradually decreases at higher temperatures indicating the similar results as discussed above.

3.3 Surface properties

The study of surface properties, such as surface tension (σ) and surface segregation (x_{Al}^S and x_{Fe}^S) provides information about the wettability, catalytic activities of alloy catalysts and other mechanical properties of liquid alloys. The surface properties of Al–Fe liquid alloy at 1873 K have been computed using Equation (12a) in the framework of Renovated Butler model. The molar surface areas of the components of the liquid alloy (λ_i ; $i = A = \text{Al}$ and $B = \text{Fe}$) are calculated from Equations (12b) and (12c) by putting

$f = 1.06$ [14, 15, 23]. The molar volume (V_i^0) of the pure component is estimated from the ratio of its atomic mass to density (m/ρ). The densities and the surface tension (σ_i^0) of the pure components of the liquid alloy are taken from Table 2.

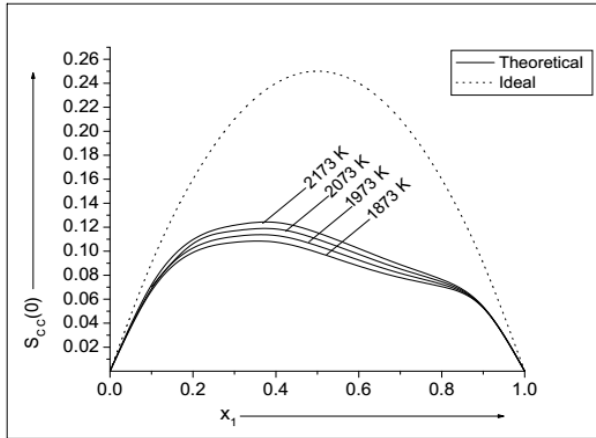


Fig. 3: The computed values of $S_{CC}(0)$ versus concentration of Al (x_1) for Al-Fe liquid alloy at different temperatures.

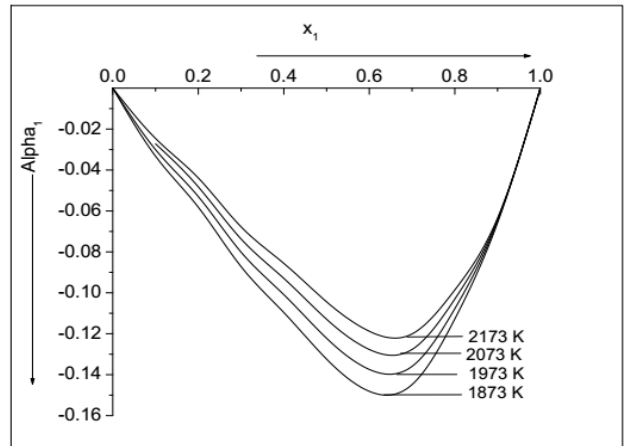


Fig. 4: The computed values of α_1 versus concentration of Al (x_1) for Al-Fe liquid alloy at different temperatures.

Table 2: densities and surface tensions of pure metals [26]

Metal	Melting temp. $T_0(K)$	Density $\rho(kg\ m^{-3})$	Surface tension $\sigma_i^0(N\ m^{-1})$
Al	933	$2385-0.280(T-T_0)$	$0.914-0.35 \times 10^{-3}(T-T_0)$
Fe	1809	$7015-0.880(T-T_0)$	$1.872-0.49 \times 10^{-3}(T-T_0)$

The computed values of σ as a function of concentration for Al-Fe liquid alloy at 1873 K are plotted in Figure 6. It can be observed that the theoretical value of σ is less than its ideal value at all concentrations. The perusal of Figure 7 communicates that the surface concentration of Al (x_{Al}^S) is greater whereas that of Fe (x_{Fe}^S) is less than their corresponding ideal values revealing that Al atoms segregates on the surface region and Fe atoms remains in the bulk region of the liquid mixture at 1873 K.

It has been already mentioned that the thermodynamic properties have been correlated with the Renovated Butler model to predict the surface properties of the preferred liquid alloys at different temperatures. The compositional dependence of σ , x_{Al}^S and x_{Fe}^S are computed at afore mentioned temperatures from Equation (12) with the aid of values from Tables 1 and 2. Figure 8 portrays the compositional dependence of σ of the system at different temperatures. The predicted value of surface tensions decreases at elevated temperatures which may due to decrease in cohesive force of the liquid mixture as forecasted by the thermodynamic and structural properties earlier.

Figure 9 shows the compositional dependence of x_{Al}^S and x_{Fe}^S for the alloy at different temperature. The computed values of x_{Al}^S gradually decreases whereas that of x_{Fe}^S gradually increases with increase in the temperatures of the melt above 1873 K. Both of these values get closure to their respective ideal values at elevated temperatures. It can be thus predicted that the Al atoms move from surface region to the bulk region whereas the Fe atoms move from bulk region to the surface region with increase in temperature of the alloy to maintain equilibrium in the liquid phase.

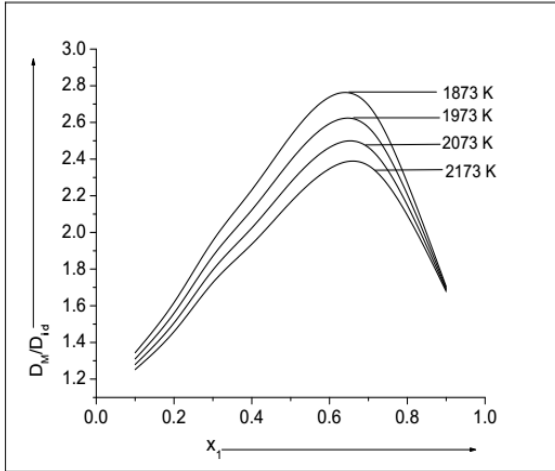


Fig. 5: The computed values of D_M/D_{id} versus concentration of Al (x_1) for Al-Fe liquid alloy at different temperatures.

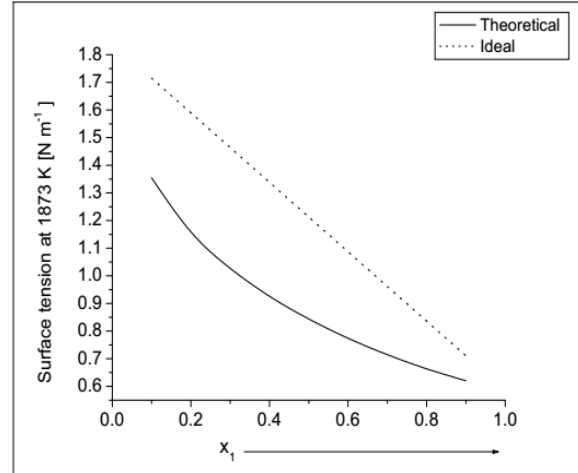


Figure 6: Surface tension (σ) versus concentration of Al (x_1) for Al-Fe liquid alloy at 1873 K.

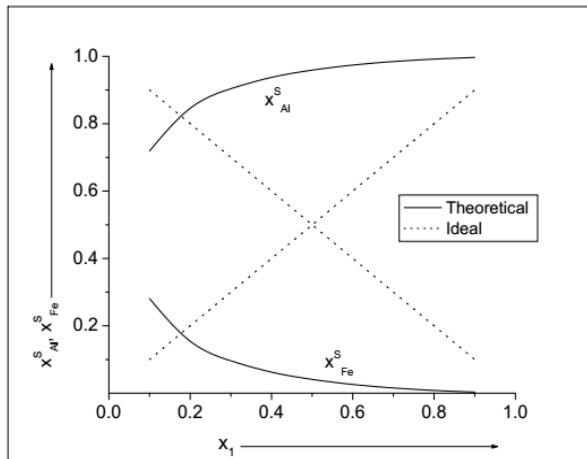


Fig. 7: The computed values of surface concentration of Al (x_{Al}^S) and Fe (x_{Fe}^S) versus concentration of Al (x_1) for Al-Fe liquid alloy at 1873 K.

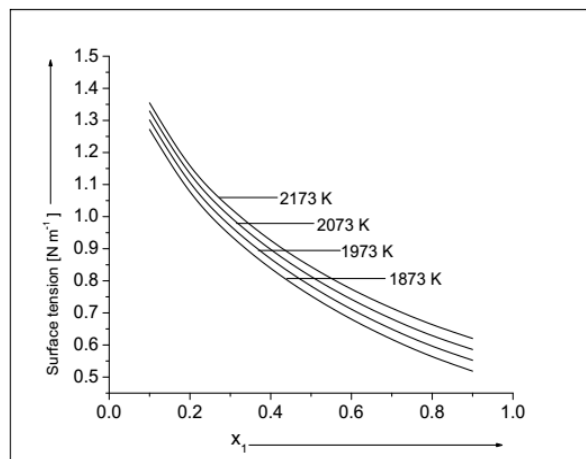


Fig. 8: The computed values of surface tension (σ) versus concentration of Al (x_1) for Al-Fe liquid alloy at different temperatures.

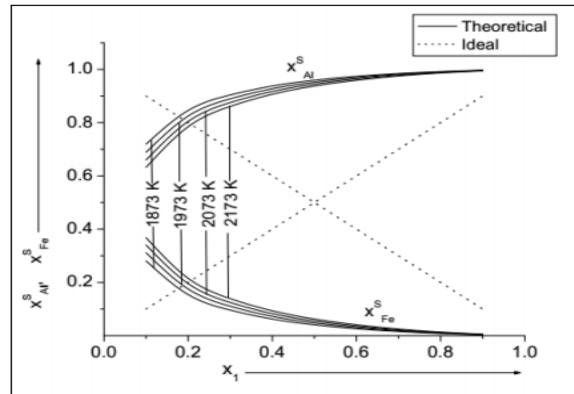


Fig. 9: The computed values of x_{Al}^S and x_{Fe}^S versus concentration of Al (x_1) for Al–Fe liquid alloy at different temperatures.

4. Conclusions

The theoretical investigations forecast that the compound forming tendency of the preferred liquid alloy gradually decreases at higher temperatures. The alloy is found to be the most reactive at its melting temperature and this nature gradually declines at elevated temperature. The surface concentrations of Al decreases whereas that of Fe increases with increase in temperature of the alloy indicating the movement of former atoms from the surface to bulk region and that of later atoms from bulk to surface region. Additionally, the system shows ideal behaviour at higher temperatures.

References

- [1] A.B. Bhatia, W.H. Hargrove, Concentration fluctuations and thermodynamic properties of some compound forming binary molten systems, *Phys. Rev. B* 10 (1974) 3186. doi.org/10.1103/PhysRevB.10.3186.
- [2] N.H. March, J.A. Alonso, Non-monotonic behaviour with concentration of the surface tension of certain binary liquid alloys, *Phys. Chem. Liq.* 46 (2008) 522. doi.org/10.1080/00319100801930466.
- [3] R. Novakovic, Thermodynamics, surface properties and microscopic functions of liquid Al–Nb and Nb–Ti alloys, *J. Non-Cryst. Solids*, 356 (2010) 1593. doi.org/10.1016/j.jnoncrsol.2010.05.055.
- [4] P.J. Flory, Thermodynamics of High Polymer Solutions, *J. Chem. Phys.* 10 (1942) 51. doi.org/10.1063/1.1723621.
- [5] D. Adhikari, I.S. Jha, B.P. Singh, Structural asymmetry in liquid Fe–Si alloys, *Phil. Mag.* 90 (2010) 2687. doi.org/10.1080/14786431003745302.
- [6] K. Hoshino, W.H. Young, On the electrical resistivity of the liquid Li–Pb alloy, *J. Phys. F: Metal Phys.* 10 (1980) 1365. doi.org/10.1088/0305-4608/10/7/003.
- [7] S.K. Yadav, L.N. Jha, D. Adhikari, Thermodynamic and structural properties of Bi-based liquid alloys *Physica B*, 475 (2015) 40. doi.org/10.1016/j.physb.2015.06.015.
- [8] H. Ruppertsberg, H.J. Reiter, A simple local pseudopotential for lithium, *J. Phys. F: Metal Phys.* 12 (1982) 1311. doi.org/10.1088/0305-4608/12/7/005.
- [9] S.K. Yadav, L.N. Jha, D. Adhikari, Thermodynamic, structural, transport and surface properties of Pb–Ti liquid alloy, *Bibechana* 13 (2016) 100. doi.org/10.3126/bibechana.v13i0.13443.
- [10] A.S. Jordan, *Metall. Trans.* 1 (1970) 239.
- [11] S. Lele, P. Ramchandrarao, Estimation of complex concentration in a regular associated solution *Metall. Met. Trans.* 12 (1981) 659. doi.org/10.1007/BF02654134.

- [12] I.S. Jha, D. Adhikari, B.P. Singh, Mixing behaviour of sodium-based liquid alloys, *Phys. Chem. Liq.*, 50 (2012) 199. doi.org/10.1080/00319104.2011.569887.
- [13] G. Kaptay, Partial Surface Tension of Components of a Solution, *Langmuir* 31 (2015) 5796. doi.org/10.1021/acs.langmuir.5b00217.
- [14] G. Kaptay, Modelling equilibrium grain boundary segregation, grain boundary energy and grain boundary segregation transition by the extended Butler equation, *J. Mater. Sci.*, 51 (2016) 1738. doi.org/10.1007/s10853-015-9533-8.
- [15] S.K. Yadav, L.N. Jha, I.S. Jha, B.P. Singh, R.P. Koirala, D. Adhikari, Prediction of thermodynamic and surface properties of Pb–Hg liquid alloys at different temperatures, *Phil. Mag.* 96 (2016) 1909. doi.org/10.1080/14786435.2016.1181281.
- [16] O. Redlich, A. Kister, Thermodynamics of Nonelectrolyte Solutions - x-y-t relations in a Binary System, *Indust. Eng. Chem.* 40 (1948) 345. doi.org/10.1021/ie50458a035.
- [17] R.N. Singh, F. Sommer, Segregation and immiscibility in liquid binary alloys, *Rep. Prog. Phys.* 60 (1997) 57. doi.org/10.1088/0034-4885/60/1/003.
- [18] D. Adhikari, S.K. Yadav, L.N. Jha, Thermo-physical properties of Al–Fe melt, *J. Chin. Adv. Mater. Soc.* 2 (2014) 149. doi.org/10.1080/22243682.2014.928603.
- [19] P. Desai, Thermodynamic Properties of Selected Binary Aluminum Alloy Systems, *J. Phys. Chem. Ref. Data*, 16 (1987) 112. doi.org/10.1063/1.555788.
- [20] I. Prigogine, R. Defay, *Chem. Thermodynamics*, Longmans Green and Co., London, 1974.
- [21] J.M. Cowley, An Approximate Theory of Order in Alloys, *Phys. Rev.* 77 (1950) 669. doi.org/10.1103/PhysRev.77.669.
- [22] L.S. Darken, R.W. Gurry, *Phys. Chem. Metals*, McGraw Hill, New York (1953).
- [23] S.K. Yadav, L.N. Jha, D. Adhikari, Theoretical Modeling to Predict the Thermodynamic, Structural, Surface and Transport Properties of the Liquid Ti–Na Alloys at different Temperatures, *J.N.P.S.*, 4 (2017) 101.
- [24] O.E. Awe, Y.A. Odusote, L.A. Hussain, O. Akinlade, Temperature dependence of thermodynamic properties of Si–Ti binary liquid alloys, *Therm. Acta*, 519 (2011) 1. doi.org/10.1016/j.tca.2011.02.028.
- [25] G. Kaptay, On the Tendency of Solutions to Tend Toward Ideal Solutions at High Temperatures *Metall. Mater. Trans. A*, 43 (2012) 531. doi.org/10.1007/s11661-011-0902-x.
- [26] E.A. Brandes, G.B. Brook, *Smithells Metals Reference Book*, Jordanhill, Oxford: Butterworth–Heinemann (1992).